

Scattering of Unidirectional Surface Waves*

S. R. SESHADRI†, SENIOR MEMBER, IEEE

Summary—A perfectly conducting plane screen embedded in a gyrotropic medium is shown to be able to support a unidirectional surface wave. Such a surface wave is assumed to be incident on the top of a semi-infinite screen. At the edge the incident power is converted partly into a reflected surface wave which travels on the bottom of the screen and partly into a space wave. The angular distribution of the radiated energy as well as the power-reflection and the power-transmission coefficients are evaluated. Total reflection is shown to occur for a certain band of frequencies.

INTRODUCTION

IN RECENT TIMES, interest has arisen in the study of scattering of electromagnetic waves by obstacles embedded in anisotropic media. Wave propagation in a homogeneous anisotropic medium is more complicated than in a homogeneous isotropic space since the characteristics of an anisotropic medium, as the name itself implies, are different in different directions. However, in general, there are two categories of problems of scattering in anisotropic media which are quite similar to those in isotropic space. The scattering by cylindrical obstacles in a uniaxially anisotropic medium constitutes the first category and Felsen [1] is currently carrying out a systematic investigation of these problems. To the second category belong certain two-dimensional problems of scattering by cylindrical obstacles in a gyrotropic medium for the case in which the gyrotropic axis is parallel to the generators of the cylinder and perpendicular to the direction of the incident wave. In this paper, a simple problem belonging to the second category is investigated.

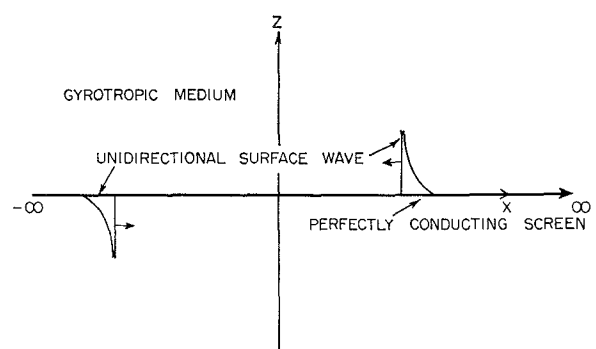
Consider a perfectly conducting screen of infinite extent embedded in a gyrotropic medium. A unidirectional surface wave has been shown [2], [3] to be supported along the screen. This surface wave is a plane TEM wave having its magnetic vector parallel and its electric vector perpendicular to the surface of the screen. The external static magnetic field is parallel to the direction of the magnetic vector of the surface wave. For a given sense of the external magnetic field, the surface wave travels only in one direction on the top of the screen and in the opposite direction on the bottom. The directions of propagation of the surface waves on the top and the bottom of the screen are both reversed when the sense of the external magnetic field is changed.

Such a unidirectional surface wave is assumed to be incident on the top of a perfectly conducting semi-

infinite screen embedded in a gyrotropic medium such that the gyrotropic axis is parallel to the edge of the screen. The unidirectional surface wave is scattered at the open end. Part of the power in the incident wave is carried by the surface wave which travels along the bottom of the screen in a direction opposite to that of the incident surface wave. The remainder of the incident power is carried by the space wave which is excited by the discontinuity. This problem is formulated in terms of a Wiener-Hopf integral equation, which is solved by the well-known function-theoretic methods. Explicit expressions for the reflection and the transmission coefficients, which give the proportion of the incident power carried, respectively, by the reflected surface wave and the transmitted space wave, are determined. For certain frequency ranges, the entire power in the incident surface wave is carried by the reflected surface wave.

UNIDIRECTIONAL SURFACE WAVES

Consider a perfectly conducting screen of infinite extent occupying the region $-\infty \leq x \leq \infty$, $-\infty \leq y \leq \infty$ and $z=0$, where x , y and z form a right-hand side rectangular coordinate system (Fig. 1). The entire space exterior to the screen is filled with a uniform plasma. A uniform magnetic field is impressed in the positive y direction throughout the plasma. Only the linear time-harmonic problem is considered and the harmonic time dependence $e^{-i\omega t}$ is suppressed. Also the treatment is restricted to the two-dimensional problem for which all the field components are independent of the y coordinate. For this case the electromagnetic field is separable into E and H modes. Since unidirectional surface waves are present only in the case of the E mode, the H mode will not be considered. For the E mode, only a



$$\vec{B} = \hat{y} B_0 \text{ FOR } 0 < \Omega < R$$

$$\vec{B} = -\hat{y} B \text{ FOR } R < \Omega < \infty$$

Fig. 1—Unidirectional surface wave along an infinite screen.

* Received March 4, 1963; revised manuscript received April 17, 1963. The research reported in this paper was supported by the National Science Foundation, Washington, D. C., Grant G 9721.

† Gordon McKay Laboratory, Harvard University, Cambridge, Mass.

single component of the magnetic field, namely H_y , is present and it can be shown [2] to satisfy the following wave equation:

$$\left[\frac{\partial^2}{\partial x^2} + \frac{\partial^2}{\partial z^2} + k^2 \right] H_y(x, z) = 0 \quad (1)$$

where

$$\begin{aligned} k^2 &= \frac{\omega^2 \mu_0 \epsilon_0 \epsilon}{\epsilon_1} = \frac{k_0^2 \epsilon}{\epsilon_1} & \epsilon &= \epsilon_1^2 - \epsilon_2^2 \\ \epsilon_1 &= \frac{\Omega^2 - R^2 - 1}{\Omega^2 - R^2}, & \epsilon_2 &= \frac{R}{\Omega(\Omega^2 - R^2)} \\ \epsilon &= \frac{(\Omega^2 - \Omega_1^2)(\Omega^2 - \Omega_2^2)}{\Omega^2(\Omega^2 - \Omega_2^2)}, & \Omega &= \frac{\omega}{\omega_p}, \quad R = \frac{\omega_c}{\omega_p} \\ \Omega_1 &= \mp \frac{R}{2} + \sqrt{\frac{R^2}{4} + 1}, & \Omega_2 &= \sqrt{1 + R^2}. \end{aligned} \quad (2)$$

In (2), k_0 is the wave number corresponding to vacuum and μ_0 and ϵ_0 are the permeability and dielectric constant pertaining to vacuum. Also ω_p and ω_c are, respectively, the plasma and the gyromagnetic frequency of an electron.

The nonvanishing components $E_x(x, z)$ and $E_z(x, z)$ of the electric field may be shown to be given by

$$\begin{aligned} E_x(x, z) &= -\frac{i\epsilon_1}{\omega\epsilon_0\epsilon} \frac{\partial}{\partial z} H_y(x, z) - \frac{\epsilon_2}{\omega\epsilon_0\epsilon} \frac{\partial}{\partial x} H_y(x, z) \\ E_z(x, z) &= \frac{i\epsilon_1}{\omega\epsilon_0\epsilon} \frac{\partial}{\partial x} H_y(x, z) - \frac{\epsilon_2}{\omega\epsilon_0\epsilon} \frac{\partial}{\partial z} H_y(x, z) \end{aligned} \quad (3)$$

In view of (1), it is reasonable to assume the following solution for $H_y(x, z)$:

$$H_y(x, z) = H_s e^{ik_x x + i\sqrt{k^2 - k_x^2} |z|} \quad (4)$$

where

$$\begin{aligned} \sqrt{k^2 - k_x^2} &= +\sqrt{k^2 - k_x^2} & \text{if } k > k_x \\ \sqrt{k^2 - k_x^2} &= +i\sqrt{k_x^2 - k^2} & \text{if } k < k_x. \end{aligned} \quad (5)$$

Since the screen is perfectly conducting, the following boundary condition has to be satisfied on the surface of the screen:

$$E_x(x, 0 \pm) = 0. \quad (6)$$

It is seen that (4) satisfies the boundary condition (6), provided

$$\epsilon_1 \sqrt{k^2 - k_x^2} = \pm i\epsilon_2 k_x \quad \text{for } z \leq 0. \quad (7)$$

With the help of (2) and (5), the solution of (7) for k_x

is easily shown to be given by

$$k_x = \pm k_0 \sqrt{\epsilon_1} \frac{|\epsilon_2|}{\epsilon_2} \quad \text{for } z \leq 0. \quad (8)$$

Hence, for $\epsilon_2 < 0$, (4) becomes

$$H_y(x, z) = H_s e^{\mp i k_0 \sqrt{\epsilon_1} r - (k_0 |\epsilon_2| |z|) / \sqrt{\epsilon_1}} \quad \text{for } z \leq 0. \quad (9)$$

It is clear that (9) represents a surface wave for the range of Ω for which $\epsilon_1 > 0$. In Fig. 2, a plot of ϵ_1 as a function of Ω is given. An examination of Fig. 2 shows that $\epsilon_1 > 0$ in the following frequency ranges:

$$0 < \Omega < R, \quad \sqrt{1 + R^2} < \Omega < \infty. \quad (9a)$$

Note that R is positive. From the expression of ϵ_1 given in (2) it is obvious that $\epsilon_1 < 0$ for the frequency range $0 < \Omega < R$ and $\epsilon_1 > 0$ for $\sqrt{1 + R^2} < \Omega < \infty$. It is clear that the sign of ϵ_1 will change if the sense of the external magnetic field is changed. It is assumed in what follows that the external magnetic field is in the positive y direction for the frequency range $0 < \Omega < R$ and in the negative y direction for $\sqrt{1 + R^2} < \Omega < \infty$. As a consequence, ϵ_1 is always negative. Therefore, $H_y(x, z)$, given by (9), holds for all Ω . For the frequency ranges $0 < \Omega < R$ and $\sqrt{1 + R^2} < \Omega < \infty$, (9) represents a surface wave. On the top ($z > 0$) of the screen, the surface wave travels in the negative x direction and on the bottom ($z < 0$) it travels in the positive x direction. For the specified orientation of the external magnetic field a surface wave which travels in the positive x direction on the top of the screen and in the negative x direction on the bottom is not obtainable. The surface waves are, therefore, unidirectional in character. Since, for the surface wave, $E_x(x, z) = 0$, it is clear that it is a TEM wave with its magnetic and electric vectors, respectively, parallel and perpendicular to the surface of the screen. The excitation of these surface waves was discussed in an earlier paper [2].

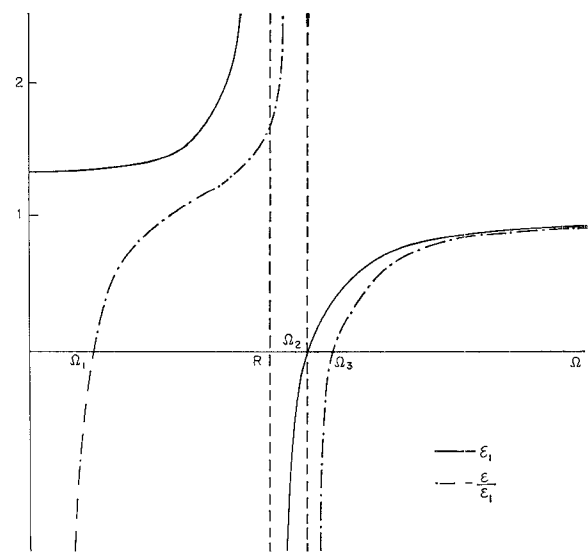


Fig. 2—Plot of ϵ_1 and ϵ_2/ϵ_1 as a function of Ω .

SCATTERING OF THE SURFACE WAVE AT THE OPEN END

It is now desired to examine the effect of terminating the perfectly conducting screen ($0 \leq x \leq \infty$) at $x=0$, on the surface wave given by (9) when it is incident on the top ($z > 0$) from $x = \infty$ (Fig. 3). No surface wave can be supported in the region $x < 0$; also, a surface wave traveling in the positive x direction cannot be supported on the top of the screen. Hence, the incident surface wave will be partly reflected back as a surface wave on the bottom and partly converted into a radiation field.

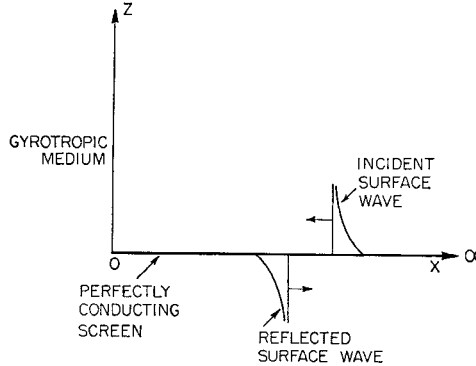


Fig. 3—Unidirectional surface wave along a semi-infinite screen.

Since only the y component of the magnetic field is present, the current $I(x)$ induced on the screen is in the x direction. When the current term is also included, it may be shown that $H_y(x, z)$ satisfies the following inhomogeneous wave equation:

$$\left[\frac{\partial^2}{\partial x^2} + \frac{\partial^2}{\partial z^2} + k^2 \right] H_y(x, z) = - \left[i \frac{\epsilon_2}{\epsilon_1} \frac{\partial}{\partial x} + \frac{\partial}{\partial z} \right] I(x) \delta(z). \quad (10)$$

The solution of (10) is easily shown to be

$$H_y(x, z) = \frac{i}{4} \left(i \frac{\epsilon_2}{\epsilon_1} \frac{\partial}{\partial x} + \frac{\partial}{\partial z} \right) \cdot \int_0^\infty I(x') H_0^{(1)} [k \sqrt{(x-x')^2 + z^2}] dx'. \quad (11)$$

Together with (3) it can be shown that, for $z=0$,

$$E_x(x, 0) = - \frac{1}{4\omega\epsilon_0\epsilon_1} \left(\frac{\partial^2}{\partial x^2} + k_0^2\epsilon_1 \right) \cdot \int_0^\infty I(x') H_0^{(1)} [k |x-x'|] dx'. \quad (12)$$

Since the perfectly conducting screen occupies only the region $x > 0$, the boundary condition (6) holds only for $x > 0$.

The application of a Fourier transformation to both sides of (12) yields

$$\bar{E}_x(\xi) = - \frac{1}{2\omega\epsilon_0\epsilon_1} \frac{(k_0^2\epsilon_1 - \xi^2)}{\sqrt{k^2 - \xi^2}} \bar{I}(\xi) \quad (13)$$

where

$$\bar{E}_x(\xi) = \int_{-\infty}^0 E_x(x, 0) e^{-i\xi x} dx \quad (14a)$$

$$\bar{I}(\xi) = \int_0^\infty I(x) e^{-i\xi x} dx. \quad (14b)$$

The branch cuts are defined as in (5).

The transform equation (13) may be solved by a straightforward application of the Wiener-Hopf procedure [4]. The result is

$$\bar{I}(\xi) = \frac{C \sqrt{k - \xi}}{k_0^2\epsilon_1 - \xi^2} \quad (15)$$

where C is a constant. With the help of (11), (14) and (15), it follows that

$$H_y(x, z) = \frac{iC}{4\pi} \int_{-\infty}^\infty \left(- \frac{\epsilon_2}{\epsilon_1} \xi \pm i\sqrt{k^2 - \xi^2} \right) \cdot \frac{e^{i\sqrt{k^2 - \xi^2}|z|} e^{i\xi x}}{(k_0^2\epsilon_1 - \xi^2) \sqrt{k + \xi}} d\xi. \quad (16)$$

In (16), the upper and lower signs hold, respectively, for z positive or negative. The contour for integration in (16) is shown in Fig. 4. For $x > 0$, the integral can be evaluated by closing the contour in the upper half-plane. For $z > 0$, the residue at the pole $\xi = k_0\sqrt{\epsilon_1}$ is seen to be zero if the fact that $\epsilon_2 < 0$ is noted. The contribution from the pole $\xi = -k_0\sqrt{\epsilon_1}$ is

$$H_y^i(x, z) = \frac{C |\epsilon_2|}{2\epsilon_1 \sqrt{k - k_0\sqrt{\epsilon_1}}} e^{-ik_0x\sqrt{\epsilon_1} - k_0(|\epsilon_2|z/\sqrt{\epsilon_1})}. \quad (17)$$

This gives just the incident surface wave (9). Hence, the constant C can be determined and it is given by

$$C = \frac{2H_s \epsilon_1 \sqrt{k - k_0\sqrt{\epsilon_1}}}{|\epsilon_2|}. \quad (18)$$

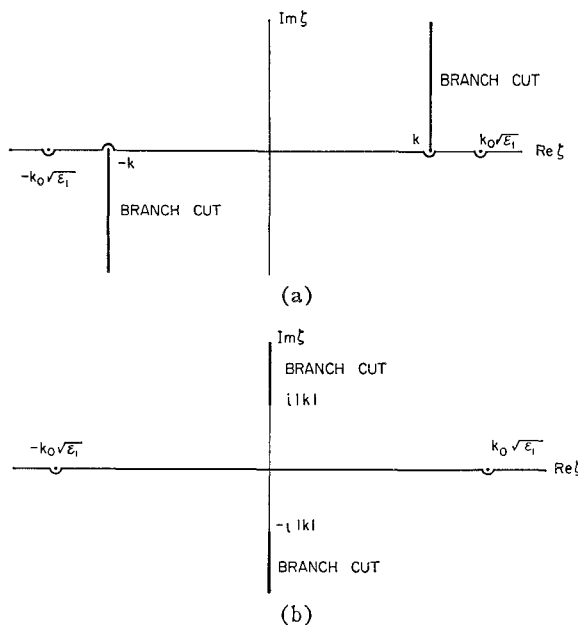
For $z < 0$, the residue at the pole $\xi = -k_0\sqrt{\epsilon_1}$ is zero and the contribution from the pole $\xi = k_0\sqrt{\epsilon_1}$ yields the reflected surface wave to be

$$H_y^r(x, z) = H_s \Gamma e^{ik_0x\sqrt{\epsilon_1} + (k_0|\epsilon_2|z/\sqrt{\epsilon_1})} \quad (19)$$

where the reflection coefficient Γ is given by

$$\Gamma = \frac{\sqrt{k - k_0\sqrt{\epsilon_1}}}{\sqrt{k + k_0\sqrt{\epsilon_1}}}. \quad (20)$$

It is desired to calculate the incident power, the power in the reflected surface wave and the power transmitted as a space wave, all per unit width of the screen. The power in the incident surface wave per unit width of the

Fig. 4—Integration contour. (a) k real. (b) k imaginary.

screen is obtained from the relation

$$\begin{aligned} P_i &= \int_0^\infty -\hat{x} \cdot \frac{1}{2} \operatorname{Re} \mathbf{E}(x, z) \times \mathbf{H}^*(x, z) dz \\ &= \frac{1}{2} \operatorname{Re} \int_0^\infty E_z^i(x, z) H_y^{i*}(x, z) dz. \end{aligned} \quad (21)$$

With the use of (9) in (3), it is found that

$$E_z^i(x, z) = \frac{k_0}{\omega \epsilon_0 \sqrt{\epsilon_1}} H_s e^{-ik_0 x \sqrt{\epsilon_1} - k_0 (|\epsilon_2|/\sqrt{\epsilon_1}) z}. \quad (22)$$

Together with (9) and (22), (21) yields

$$P_i = \frac{|H_s|^2}{4\omega\epsilon_0 |\epsilon_2|}. \quad (23)$$

In a similar way, the power transmitted in the reflected surface wave per unit width of the screen is

$$P_r = \frac{|H_s|^2 |\Gamma|^2}{4\omega\epsilon_0 |\epsilon_2|}. \quad (24)$$

The reflection coefficient S is, therefore, given by

$$S = \frac{P_r}{P_i} = |\Gamma|^2 = \frac{\epsilon_1 - \sqrt{\epsilon}}{\epsilon_1 + \sqrt{\epsilon}} \quad \text{for } k \text{ real.} \quad (25)$$

The power radiated in the form of a space wave can be evaluated in the following manner. For this purpose, it is convenient to introduce the polar coordinates

$$x = \rho \cos \theta, \quad z = \rho \sin \theta \quad (26)$$

and the following transformation:

$$\xi = k \cos \gamma. \quad (27)$$

With (26) and (27), (16) reduces to

$$H_y(\rho, \theta) = -\frac{iCk^2}{4\pi} \int \left(-\frac{\epsilon_2}{\epsilon_1} \cos \gamma + i \sin \gamma \right) \frac{e^{ik\rho \cos(\gamma-\theta)} \sin \gamma d\gamma}{[k_0^2 \epsilon_1 - k^2 \cos^2 \gamma][k + k \cos \gamma]^{1/2}}. \quad (28)$$

For $k\rho \gg 1$, (28) is evaluated by the saddle-point method. It yields the space wave part as follows:

$$H_y^R(\rho, \theta) = -\frac{iCk^2}{2\sqrt{2\pi k\rho}} \frac{\left(-\frac{\epsilon_2}{\epsilon_1} \cos \theta + i \sin \theta \right) \sin \theta}{(k_0^2 \epsilon_1 - k^2 \cos^2 \theta)(k + k \cos \theta)^{1/2}} \cdot e^{i(k\rho - \pi/4)}. \quad (29)$$

With (3) and (26) it may easily be shown that, for $k\rho \gg 1$,

$$E_\theta(\rho, \theta) \simeq -\frac{\epsilon_1 k}{\omega \epsilon_0 \epsilon} H_y(\rho, \theta). \quad (30)$$

The outward power flow per unit area per unit length of the screen at angle θ is obtained from (29) and (30) as

$$\begin{aligned} S^R &= \frac{1}{2} \operatorname{Re} \hat{\mathbf{E}}(\rho, \theta) \times \mathbf{H}^*(\rho, \theta) = \frac{k\epsilon_1}{2\omega\epsilon_0\epsilon} |H_y(\rho, \theta)|^2 \\ &= \frac{\epsilon |C|^2 F(\theta)}{16\pi\rho\omega\epsilon_0\epsilon^3} \end{aligned} \quad (31)$$

where

$$F(\theta) = \frac{(1 - \cos \theta)}{\left[1 - \frac{\epsilon}{\epsilon_1^2} \cos^2 \theta \right]}. \quad (32)$$

$F(\theta)$, given in (32), is defined as the radiation pattern. The total power P^R radiated in the form of space waves is

$$P^R = \int_0^{2\pi} S^R \rho d\theta = \frac{\epsilon |C|^2}{16\pi\omega k\epsilon_0\epsilon^3} \int_0^{2\pi} F(\theta) d\theta. \quad (33)$$

It can be readily shown that, for $F(\theta)$ in (32),

$$\int_0^{2\pi} F(\theta) d\theta = \frac{2\pi\epsilon_1}{|\epsilon_2|}. \quad (34)$$

The use of (18) and (34) in (33) yields, after some simplification,

$$P^R = \frac{|H_s|^2 \sqrt{\epsilon}}{2\omega\epsilon_0 |\epsilon_2| (\epsilon_1 + \sqrt{\epsilon})}. \quad (35)$$

The transmission coefficient T , which is defined as the ratio of the power radiated as a space wave to the incident power (both per unit width of the screen), is, therefore,

$$T = \frac{P^R}{P_i} = \frac{2\sqrt{\epsilon}}{\epsilon_1 + \sqrt{\epsilon}} \quad \text{for } k \text{ real.} \quad (36)$$

It may be verified from (25) and (36) that $S+T=1$, as it should.

Since (25) and (36) are valid only for k real, it is pertinent to find out the ranges of Ω for which k is real. It is easily established that $\Omega_1 < R < \Omega_2 < \Omega_3$. From (2), it is obvious that $\epsilon/\epsilon_1 > 0$ only in the frequency ranges $\Omega_1 < \Omega < \Omega_2$ and $\Omega_3 < \Omega < \infty$ (Fig. 2). Hence, the expressions for the reflection coefficient, the radiation pattern and the transmission coefficient, given, respectively, in (25), (32) and (36), are valid only for $\Omega_1 < \Omega < \Omega_2$ and $\Omega_3 < \Omega < \infty$. The incident surface wave assumed in (9) is legitimate only for the frequency ranges defined in (9a). Therefore, Ω is also restricted to these ranges. Within the stipulated ranges of Ω , ϵ/ϵ_1 and, hence, k^2 are negative in the ranges $0 < \Omega < \Omega_1$ and $\Omega_2 < \Omega < \Omega_3$. For k purely imaginary the solution of (13) has to be modified, with the result in the final solution (15), k should be replaced by $i|k|$. Then it is obvious from (20) and (25) that

$$S = 1 \quad (37)$$

for $0 < \Omega < \Omega_1$ and $\Omega_2 < \Omega < \Omega_3$. When k in (29) is replaced by $i|k|$, it is seen that the space wave is exponentially damped and, hence, no power is radiated in the form of a space wave. Hence,

$$T = 0 \quad (38)$$

for $0 < \Omega < \Omega_1$ and $\Omega_2 < \Omega < \Omega_3$. The power in the incident surface wave traveling on the top of the screen is totally reflected as a surface wave which travels on the bottom of the screen when Ω is in the ranges $0 < \Omega < \Omega_1$ and $\Omega_2 < \Omega < \Omega_3$.

NUMERICAL RESULTS

The reflection and the transmission coefficients are computed as a function of Ω for a particular value of R , namely, $R = \sqrt{3}$. It is seen from an examination of Fig. 5 that the reflection coefficient is unity from $0 < \Omega < \Omega_1$; it falls off rapidly as Ω is increased beyond Ω_1 , reaches a minimum and then increases to unity at $\Omega = R$. It starts again at unity when $\Omega = \Omega_2$ and remains at that value for Ω up to Ω_3 ; then it quickly falls to zero as Ω is increased beyond Ω_3 . It is obvious that in the frequency ranges for which the reflected surface wave and the space wave are present, the major portion of the energy is transmitted as a space wave except for Ω very near Ω_1 , R and Ω_3 . For a certain frequency between Ω_1 and R , the transmission coefficient has a maximum and, in the frequency ranges considerably greater than Ω_3 , a negligible amount of incident power is reflected as a surface wave.

The radiation pattern $F(\theta)$, given in (32), is plotted in Fig. 6 for $R = \sqrt{3}$ and for three values of Ω . It is found that the radiation pattern always has a null in the direction of the screen and a maximum in the opposite direction. It is found that, for $\Omega > \Omega_3$, the maximum increases very rapidly with Ω , as can be seen

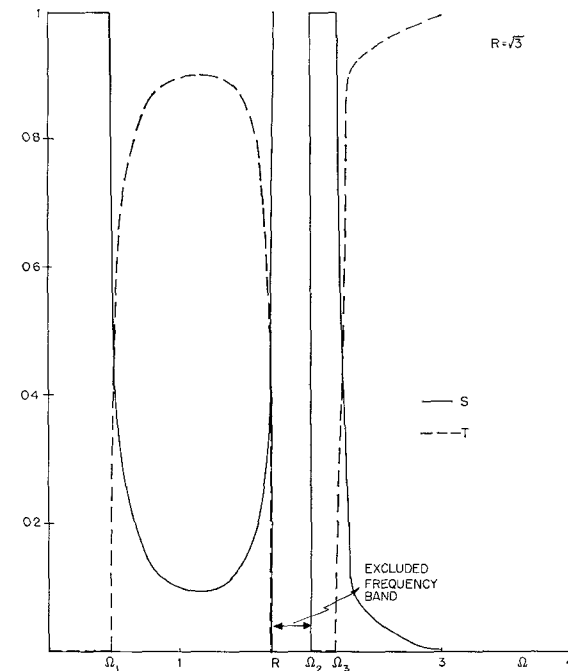


Fig. 5—Reflection and transmission coefficients.

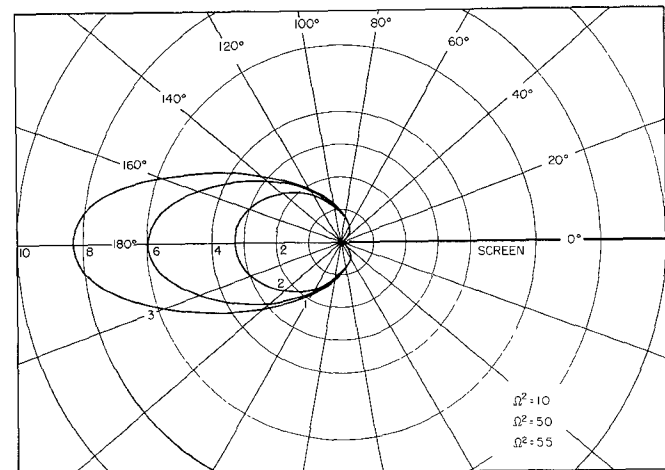


Fig. 6—Radiation pattern.

from the patterns for $\Omega^2 = 5$ and $\Omega^2 = 5.5$. For example, when $\Omega = 3$, the maximum value is nearly 20 times larger than that for $\Omega = \sqrt{5.5}$. The reason for this rapid change in the maximum in the radiation pattern can be explained in the following manner. For $\Omega > \Omega_3$, the reflection coefficient S falls off very rapidly as Ω is increased beyond Ω_3 . Hence, the major portion of the incident power is transmitted as a space wave. Also, as Ω is increased beyond Ω_3 , ϵ_2 rapidly decreases to a very small value. As a consequence, the exponential attenuation in the incident plane wave is rapidly reduced. The incident wave becomes very nearly a homogeneous plane wave and, therefore, the total incident power increases sharply when Ω is increased further. Since the major portion of the incident power is transmitted as a space

wave, the maximum in the radiation pattern rises sharply as Ω is increased beyond Ω_3 .

ACKNOWLEDGMENT

The author wishes to thank Prof. R. W. P. King for reading the manuscript. He is grateful to Prof. L. B. Felsen who made possible the author's visit to the Polytechnic Institute of Brooklyn, Brooklyn, N. Y., where this work was done. He is also thankful to Profs. A. A. Oliner and L. B. Felsen for their helpful discussions.

REFERENCES

- [1] L. B. Felsen, "On Diffraction by Objects in a Uniaxially Anisotropic Medium," Polytechnic Institute of Brooklyn, Brooklyn, N. Y., Memo. No. 83, PIBMRI-1073-62; August, 1962.
- [2] S. R. Seshadri, "Excitation of surface waves on a perfectly conducting screen covered with anisotropic plasma," IRE TRANS. ON MICROWAVE THEORY AND TECHNIQUES, vol. 10, pp. 573-578; November, 1962.
- [3] A. Ishimaru, "The Effect of a Unidirectional Surface Wave Along a Perfectly Conducting Plane on the Radiation from a Plasma Sheath," presented at the Second Symp. on the Plasma Sheath, Boston, Mass.; April, 1962.
- [4] S. R. Seshadri, "Scattering of Unidirectional Surface Waves," No. 402, Cruft Lab., Harvard University, Cambridge, Mass., Tech. Rept. No. 402; February, 1963.

Attenuation Constant of Lunar Line and *T*-Septate Lunar Line*

A. Y. HU†, MEMBER, IEEE, AND A. ISHIMARU‡, SENIOR MEMBER, IEEE

Summary—The attenuation constant α of the lunar line and that of the *T*-septate lunar line were derived from the average power loss W_L and the average power transfer W_T in each line, that is the ratio, $W_L/2W_T$. The average power loss and the average power transfer for the lunar line and for the *T*-septate lunar line were derived from their respective field functions. The theoretical attenuation constant of a typical lunar line is less than 0.7 db/100 ft for frequencies greater than 2000 Mc. The theoretical attenuation constant of a typical *T*-septate line is less than 0.9 db/100 ft for frequencies greater than 1000 Mc. Experimental measurements of the attenuation constant of a *T*-septate lunar line agree with the theoretical value. In the 200 to 2000 Mc frequency band, the lunar line and the *T*-septate lunar line offer a compact and light package without an appreciable sacrifice in peak power handling capacity or attenuation.

INTRODUCTION

TWO NEW microwave transmission lines, lunar line and *T*-septate lunar line were developed at The Boeing Company. The lunar line is an eccentric version of Schelkunoff's coaxial cylinders with a radial baffle¹ and is formed by two eccentric circular metal tubes, which are either connected with a metal bar or tangential to each other. The *T*-septate or lazy-*T* lunar line is a modification of the lunar line and is also formed by two eccentric circular metal tubes. In the *T*-septate lunar line, however, part of the inner tube is cut out and a vertical metal bar is passed through the

cut out section to connect the inner surfaces of the two tubes. The outer tube and the bar are made of brass, but the inner tube is made of copper which maintains the cylindric form after being cut. A perturbation method is used to obtain the dominant cutoff wavelength and the field functions of these lines.^{2,3}

The main effect of the finite conductivity in the waveguide will be attenuation caused by the power loss in the conducting boundaries. The value of this attenuation may be estimated by the ratio of power loss per unit length to the average power transferred. For a good conductor, it is reasonable to assume that the expression for power transfer derived for the ideal guide applies well enough to the actual guide, and that power loss may be computed by taking the current flow of the ideal guide as flowing in the walls of the actual guide with a known conductivity.

In this paper, the attenuation constant α of the lunar line and of the *T*-septate lunar line are derived from the average power loss per unit length W_L and the average power transfer for the lunar line and for the *T*-septate lunar line with their respective field functions. The numerically calculated dissipative attenuation constants of the *T*-septate lunar line for different frequencies are consistent with experimental results. Com-

* Received September 20, 1963; revised manuscript received April 18, 1963. The work was performed under Contract No. AF 19(604)-6189 with the Air Force Cambridge Research Center, Mass.; Final Report, Boeing Document D6-9043, Section 8, June, 1962.

† The Boeing Company, Transport Division, Renton, Wash.

‡ Department of Electrical Engineering, University of Washington, Seattle, Wash.

¹ S. A. Schelkunoff, "Electromagnetic Waves," D. Van Nostrand Company, Inc., New York, N. Y., p. 392; 1943.

² A. Y. Hu and A. Ishimaru, "The Dominant Cut-Off Wavelength of a Lunar Line," The Boeing Co., Seattle, Wash., Tech. Rept. No. 1, Contract No. AF 19(604)-6189, AFCRL 133, Boeing Doc. D6-7467; published in IRE TRANS. ON MICROWAVE THEORY AND TECHNIQUES, vol. MTT-9, pp. 552-556; November, 1961.

³ A. Y. Hu and D. E. Isbell, "The Dominant Cut-Off Wavelength of a *T*-Septate Lunar Line," The Boeing Co., Seattle, Wash., Tech. Rept. No. 3, Contract No. AF 19(604)-6189, AFCRL-62-80, Boeing Doc. D6-8188; January, 1962.